Journal of Constructional Steel Research 164 (2020) 105813

Contents lists available at ScienceDirect

Journal of Constructional Steel Research

journal homepage: www.elsevier.com/locate/ijcard

An experimentally verified new approach for web crippling design of cold-formed steel Z-Sections

Anwar Badawy Badawy Abu-Sena*, Fathy Abdelmoniem Abdelfattah, Mohamed Salah Soliman, Mohamed Saied Refaee Saleh

Faculty of Engineering (Shoubra), Benha University, Egypt

ARTICLE INFO

Article history:
Received 24 June 2019
Received in revised form
30 September 2019
Accepted 17 October 2019

Keywords:
Web crippling
Z-Section
Cold formed
Design codes
Analytical approach

ABSTRACT

This research aims at developing a new simple but rational analytical model to predict web crippling strength of cold formed steel Z beams. Results of the developed analytical model were verified experimentally and numerically utilizing the finite element non-linear analysis. Web crippling strengths obtained by the proposed analytical model, tests and numerical analysis were compared to the corresponding strength calculated by the equations of AISI-2016 and Eurocode 1−3. Both codes adopt empirical equations for estimating the web crippling resistance.

Comparison showed that, the predicted web crippling strength using the developed model compare well with the experimentally and numerically calculated strength. On the other hand, it was found that the design equations adopted by the AISI-2016 and Eurocode 1−3 overestimate the web crippling strength compared to the experimental and analytical strength. Accordingly, it is recommended to adopt the proposed equation as a rational formula for estimating web crippling strength of cold formed Z-sections.

1. Introduction

Web crippling is a common failure mode in cold formed steel sections due to the thin gauge steel. It occurs at locations of concentrated loads, where it is not practical to install web stiffeners. Web crippling failure is a combination of web buckling and yielding in web thickness over the extended loaded area. There is a set of factors that contribute in defining the web crippling strength of cold formed steel sections, such as; cross section geometry, loading length and location, material yield stress and fastening conditions. Numerous researches and reports were carried out to study the web crippling of cold formed steel sections. Most of these researches are experimental, because the theoretical analysis is very complicated due to the above mentioned factors that need be considered. Recently, there are many trials by the researchers to develop analytical solutions for estimating the web crippling strength instead of the current empirical design formulae. However, theoretical study of web crippling phenomena in cold formed steel section is still very complicated, that is due to, the too many parameters that need to be considered in the analysis. These parameters are summarized by Yu and LaBoube [1], as listed below:

- Non-uniform stress distribution under concentrated load.
- Local yielding at loaded area.
- Eccentric loading on web.
- Web flange restraining conditions, and
- Presence of Initial web imperfection.

There were some attempts by Young and Hancock [2,3], and Ren [4] to develop design expressions for web crippling strength in cold formed C-sections based on plastic hinge mechanisms. Bakker and Stark [5] developed an analytical model for web crippling at interior supports of continuous hat and deck sections on the bases of experimental research. Bakker and Stark defined two types of web crippling failure modes on bases of inside bend radius. The two failure modes are; the arc yield mode occurring in sections with small bend radius and rolling mode occurring in sections with large bend radius. Chen et al. [6] investigated the web crippling of cold formed steel lipped channels under four loading conditions and proposed design equations for estimating the web crippling load under the four loading conditions on bases of test results and extended verified finite element results. In their proposed design equations, the effect of corner bend radius was ignored.

Dara and Yu [7] developed a semi-analytical model to predict

* Corresponding author.
E-mail address: abbadawy@yahoo.com (A.B. Badawy Abu-Sena).

https://doi.org/10.1016/j.jcsr.2019.105813
0143-974X/

Nomenclature

EOF	End One Flange
IOF	Interior One Flange
ETF	End Two Flanges
ITF	Interior Two Flange
h	Flat web height
h_w	Web depth between mid-flanges thickness
t	Web thickness
N	Bearing plate length
R	Inside bend radius
P_n	Nominal web crippling strength
C, C_N, C_R &C_h	Web crippling coefficients
F_y	Yield stress
F_u	Ultimate stress
ε_u	Ultimate strain
R_{wd}	Web crippling resistance
k, k_1, k_2, k_3, k_4 & k_5	Web crippling coefficients
θ	Vertical web inclined
D	Overall web depth
b	Overall flange width
ds	Overall lip depth
a	Maximum out of plan displacement, mm
B	Plate width at the location of maximum out of plane displacement, Fig. 13
e	The eccentricity of the applied load = (R + t/2) mm
E	Young's modulus of steel, = 210 kN/mm^2
I	Second moment of area of the effective web section = B t^3/12, mm^4
G	Shear modulus of steel = 81 kN/mm^2
J	Torsion constant for lipped flange = (ds + b −4(R + t) + π (R + t/2)) t^3/3 mm^4
L	Equivalent beam span for torsional rigidity = N+2 h or specimen length
M_o	Moment due to eccentric applied load = (P.e) kN.mm
P	Applied load, kN
K_t	Rotational stiffness

the web crippling of C- section under IOF loading conditions and Z sections under EOF loading conditions. Dara and Yu used the direct strength method DSM concept to develop the semi-analytical model. DSM assumed that the ratio of the nominal strength/yield load is controlled by the square root of the value of yield load divided by the elastic buckling load. The proposed DSM design equations are based on the above mentioned assumptions and using curve fitting methods.

As discussed above, most of researchers focused on studying the web crippling of cold formed steel C sections under the four loading conditions. On the other hand, limited researchers studied the web crippling of cold formed steel Z-sections as surveyed by Beshara and Schuster [8]. Gerges and Schuster [9] investigated the web crippling of C-sections with large inside bend radius under end one flange loading conditions. Gerges and Schuster proposed new coefficients for EOF design expressions of North American cold formed steel design standard. Macdonald and Heiyantuduwa [10] developed a new design expressions for predicting the web crippling strength of cold formed lipped steel channel. The developed design expressions were based on results from tests and validated finite element models. Natário et al. [11] presented a computational modeling of flange crushing in cold formed steel sections subjected to ITF loading. Natário et al. pointed out that flange crushing behaviour may occur before web crippling failure mode in case of narrow bearing width. Rhodes and Nash [12] investigated theoretically the web crushing of cold formed steel plain and lipped channels due to ITF and IOF loading conditions. Their investigation firstly employed the finite element analysis to obtain the critical buckling load, thereafter; the energy approach was used in web crushing analysis. Rhodes and Nash observed that, web crushing load of lipped channels is greater than web crushing load of plain channels.

In Refs. [2,4,16,18] the web crippling of plain cold formed steel channels was investigated under the four loadings (EOF, IOF, ETF and ITF) and the experimental results were compared to the north American standard NAS-2001b. It was concluded that, the North American standard is not conservative for EOF and IOF loadings.

In Ref. [19] the web crippling test results for unstiffened unfastened C-section under IOF and ITF loadings were compared to Eurocode 3 part 1–3 (CEN 2006) and the American standard AISI 2007. It was observed that, the both standards are not conservative for estimating the web crippling strength for IOF and ITF loadings.

T. Misiek, A. Belica [20] presented an empirical design approach for C and Z sections in form of generalized equation calibrated to comply with the safety concept described in EN 1990. The generalized equation is similar to the unified design expression used in the American standard AISI-2016 with minor differences.

Lavan Sundararajah et al. [21] investigated the web crippling of cold formed lipped channel beams under ETF and ITF loadings. This investigation included experimental work and numerical finite element analysis. The web crippling tests conducted were based on the new AISI S909 standard test method for LCBs under ETF and ITF load cases. Comparison of the ultimate web crippling capacities showed that the current AISI S100 (AISI, 2012) and AS/NZS 4600 (SA, 2005) design equations are very un-conservative for LCBs under ETF load case, but are overly conservative for ITF load case. New improved design rules were proposed in that study.

Lavan Sundararajah et al. [22] investigated the web crippling of high strength lipped channel beams LCB under EOF and IOF loading conditions using the AISI standard web crippling test method. Comparisons with experimental web crippling capacities showed that AS/NZS 4600 and AISI S100 design strengths are unconservative for EOF load case and agree well in case of IOF loading. While web crippling capacities according to Eurocode 3 Part 1–3 are overly conservative for EOF and IOF load cases.

Y. Lian, A. Uzzaman et al. [23,24], experimentally investigated the effect of web holes on the web crippling strength of cold formed steel lipped channels under EOF and IOF load cases respectively. The tests included fastened and un-fastened flange specimens. Finite element models have been developed and verified against the experimental results in term of web crippling failure loads and deformations. The verified models developed to do extended parametric studies and give design recommendations.

L. Sundararajah, M. Mahendran, P. Keerthan [25] conducted experimental and numerical studies on web crippling behavior of SupaCee sections under one flange loading cases. The sections flanges were un-fastened to support. Experimental and finite element analysis results showed that the web crippling capacities of SupaCee sections are reduced relative to lipped channel sections. Suitable web crippling coefficients were proposed to be adopted in the American and Australian/New Zealand cold-formed steel design standards.

In the current research, an analytical model were developed to help the designer engineer to accurately predict the web crippling

ultimate load for cold formed Z-section using a simple but rational formula. This model was based on the deformed shape obtained from experiments and verified by finite element analysis, it also accounted for the presence of web initial imperfection. The results of the developed analytical model were verified against the experimental numerical results, and a good agreement was noticed. Results of the developed model along with the numerical and experimental results were compared to the codes design equations.

2. Current design standards

In this research, two design standards are considered; the north American specification **AISI S100-16** [13], and the Eurocode 3 Part 1–3 **EN 1993-1-3** [14]. In both design standards, the web crippling resistance is clarified into four loading conditions; Exterior One Flange (EOF), Interior One Flange (IOF), Exterior Two Flanges (ETF) and Interior Two Flanges (ITF). In the Eurocode, there are one or two design expressions including three coefficients for estimating the web crippling resistance for each loading case. In AISI S100-16, there is a unique design expression including four coefficients for estimating the web crippling strength for each cross loading case. The design equations used by the two codes for single web sections subjected to web crippling under IOF loading are given below.

2.1. AISI S100-16

According to this design code; the nominal web crippling strength of cold formed steel sections is calculated using the following design equation provided that, $h/t \le 200$, $N/t \le 210$, $N/h \le 2.0$ and $\theta = 90°$;

$$P_n = C.t^2.F_y.Sin\,\theta\left(1 - C_R\sqrt{\frac{R}{t}}\right).\left(1 + C_N\sqrt{\frac{N}{t}}\right).\left(1 - C_h\sqrt{\frac{h}{t}}\right) \quad (1)$$

where; P_n is the nominal web crippling strength, t is the web thickness, F_y is the material yield stress, R is the inside bend radius, N is the loading length, h is the flat web height and θ is the web inclination angel. The coefficients C, C_R, C_N and C_h are defined in Table 1.

2.2. EN 1993-1-3

According to this design code, for a cross-section with a single un-stiffened web, the local transverse resistance of the web may be determined as specified in the following expressions, provided that, $h/t \le 200$, $R/t \le 6$ and $45° \le \theta \le 90°$.

For sections with stiffened flanges subjected to EOF loading, the web resistance is;

$$R_{Wd} = k_1.k_2.k_3.t^2.F_y\left(9.04 - \frac{h_w/t}{60}\right).\left(1 + 0.01\frac{N}{t}\right) \quad (2.a)$$

For sections with un-stiffened flanges subjected to EOF loading, the web resistance is;

$$R_{Wd} = k_1.k_2.k_3.t^2.F_y\left(5.92 - \frac{h_w/t}{132}\right).\left(1 + 0.01\frac{N}{t}\right) \quad For\ N/t \le 60 \quad (2.b)$$

$$R_{Wd} = k_1.k_2.k_3.t^2.F_y\left(5.92 - \frac{h_w/t}{132}\right).\left(0.71 + 0.015\frac{N}{t}\right) \quad For\ N/t \le 60 \quad (2.c)$$

For sections subjected to IOF loading, the web resistance is given by:

$$R_{Wd} = k_3.k_4.k_5.t^2.F_y\left(14.7 - \frac{h_w/t}{49.5}\right).\left(1 + 0.007\frac{N}{t}\right) \quad For\ N/t \le 60 \quad (3.a)$$

$$R_{Wd} = k_3.k_4.k_5.t^2.F_y\left(14.7 - \frac{h_w/t}{49.5}\right).\left(0.75 + 0.011\frac{N}{t}\right) For\ N/t \le 60 \quad (3.b)$$

For sections subjected to ETF loading, the web resistance is given by;

$$R_{Wd} = k_1.k_2.k_3.t^2.F_y\left(6.66 - \frac{h_w/t}{64}\right).\left(1 + 0.01\frac{N}{t}\right) \quad (4)$$

For sections subjected to ITF loading, the web resistance is;

$$R_{Wd} = k_3.k_4.k_5.t^2.F_y\left(21.0 - \frac{h_w/t}{16.3}\right).\left(1 + 0.0013\frac{N}{t}\right) \quad (5)$$

where;

$$k = F_y/228 \quad (6.a)$$

$$k_1 = 1.33 - 0.33\,k \quad (6.b)$$

$$k_2 = 1.15 - 0.15\,R/t\ 0.5 \le k_2 \le 1.0 \quad (6.c)$$

$$k_3 = 0.7 - 0.3\,(\theta/90)^2 \quad (6.d)$$

$$k_4 = 1.22 - 0.22\,k \quad (6.e)$$

$$k_5 = 1.06 - 0.06\,R/t\ k_5 \le 1.0 \quad (6.f)$$

Table 1
Web crippling coefficients of single web Z-sections un-fastened to support [13].

Load patterns	Stiffened flanges				Un-Stiffened flanges			
	C	C_R	C_N	C_h	C	C_R	C_N	C_h
EOF	5	0.09	0.02	0.001	4	0.40	0.60	0.03
IOF	13	0.23	0.14	0.01	13	0.32	0.10	0.01
ETF	13	0.32	0.05	0.04	2	0.11	0.37	0.01
ITF	24	0.52	0.15	0.001	13	0.47	0.25	0.04

3. Experimental investigation

The test program has been designed to study the effect of variation of cross section geometrical properties and bearing plate widths. The considered cross section parameters are; web thickness **t**, web full depth **D** and the load bearing plate width **N** as defined in Fig. 1. The tests carried out in this research for web crippling under IOF loading conditions as defined by the Eurocode **EN 1993-1-3** [14].

The test specimens set up was simple beam loaded through bearing plate at mid span and un-fastened to supports or loading plates. As recommended by Macdonald and Heiyantuduwa [10], the web of specimens have been strengthened at support locations

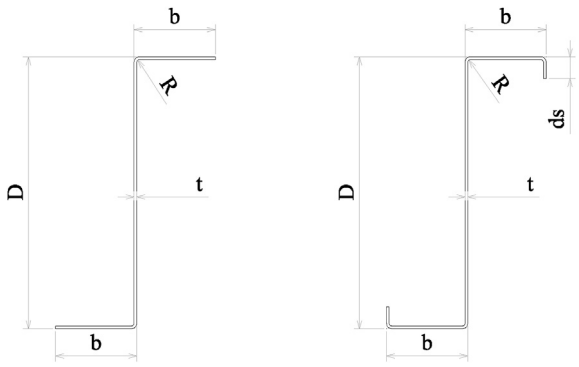

Fig. 1. Stiffened and unstiffened Z sections geometries considered in tests.

with wooden blocks as shown in Fig. 2, to make sure that web crippling failure occurs under the loading plate at mid span of test specimen and achieve the IOF loading conditions for web crippling. The end bearing plates of test specimens at support locations have a constant width of 100 mm while the loading plates have been fabricated with three different widths; 30, 50 and 100 mm.

Table 2, defines the test specimens cross section dimensions, length and loading plate widths. The specimens have been labeled such that; the cross-section shape, dimensions and loading plate width are defined as per the following example.

Z150×60×15×1.0-R2-N30

- Loading plate width (N) = 30 mm
- Inside bent radius (R) = 2 mm
- Web thickness (t) = 1.0 mm
- Lip full depth (ds)= 15 mm
- Flange full width (b) = 60 mm
- Web Full depth (D) = 30 mm
- Cross section shape is "Z"

The material properties of the test specimens were determined by tensile coupon tests. Three coupon tests were prepared according to ASTM A370 for the tensile testing of metals using 12.5 mm wide coupons of gauge length 50 mm. The coupon tests were carried out using the universal testing machine LLOYD-LR 300 K.

Table 2
Coupon test results.

t, mm	F_y, N/mm^2	F_u, N/mm^2	εu %
1.0	298	373	25.1
1.5	345	414	28.0
1.9	398	457	22.1

Table 2 summarizes the material properties determined from the coupon tests; the yield stress F_y, ultimate stress F_u and the elongation after fracture (ε_u) based on a gauge length of 50 mm. Fig. 3 shows the test specimen during coupon test.

During the tests, several measurements have been recorded such as; the applied testing load, the lateral displacement of the web in addition to the vertical movement of the bottom flange at mid span loading location. Fig. 4 shows the web crippling failure in test specimen and the measuring tools for web deformations.

4. Numerical investigation

The finite element package ANSYS [15] was used in this investigation to simulate the tested cold formed steel Z-sections for web crippling under IOF loading conditions. It is aimed to present simple accurate finite element models for the tested specimens subjected to pure web crippling. The finite element models were verified against the test results to be used in future extensive parametric study for wide range of Z-section geometries. The measured cross section dimensions, material properties, loading and boundary conditions from tests were used in building the finite element models. In finite element models, the Z-section geometries were based on centerline dimensions of cross section.

A thin shell element type "Shell181" was utilized in the finite element models to simulate the test specimens. This element is four-node element and has six degrees of freedom at each node. It is suitable for thin walled sections and has nonlinear capabilities

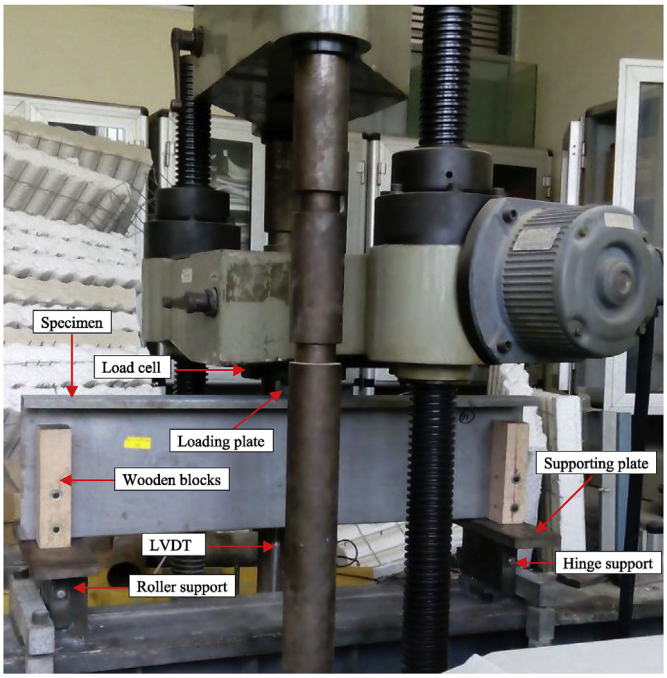

Fig. 2. Test setup for IOF loading conditions.

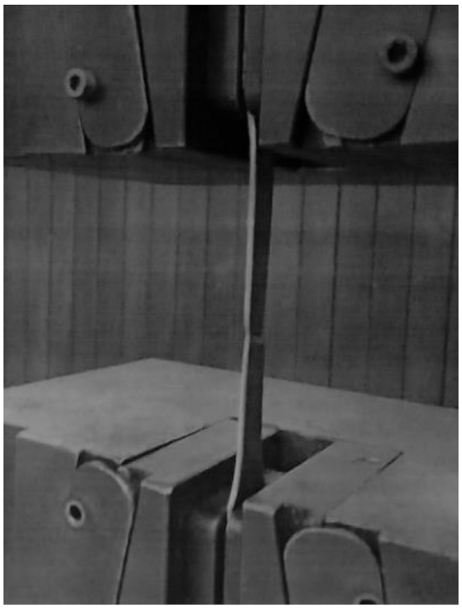

Fig. 3. Coupon test specimen.

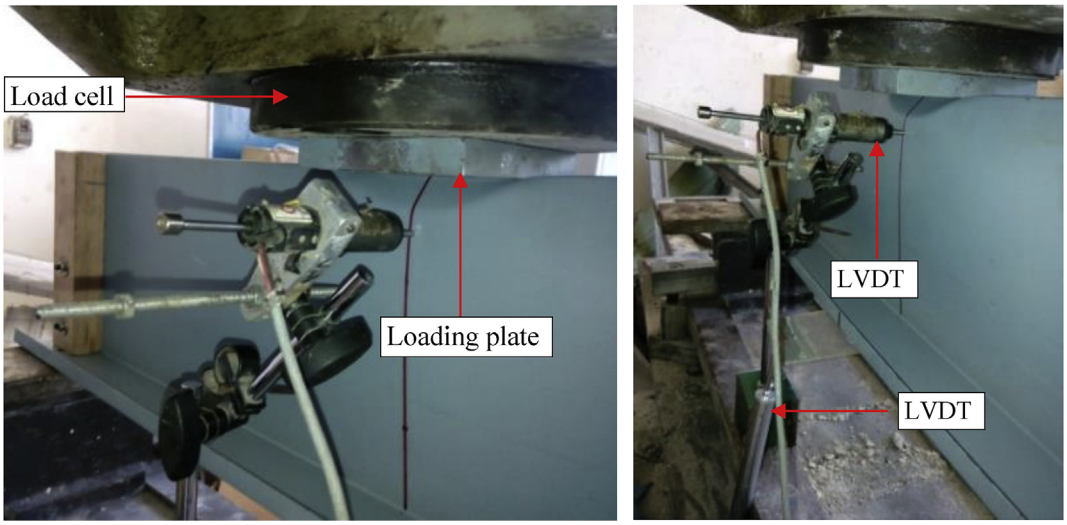

Fig. 4. Web crippling failure under IOF loading.

account for plasticity and large deformations [15].

The finite element mesh in the models has been carried out by varying the element size along the specimen length and cross section. A mesh size of approximately 5 × 5 mm have been utilized for flat flanges and lips while a mesh size of approximately 2.5 × 2.5 mm have been utilized for flat web under loading plate to simulate the web crippling deformation. A finer mesh size has been utilized at each rounded corner of Z cross sections by dividing it into four elements along the cross section. The typical arrangement for finite element models of cold formed steel Z-sections subjected to IOF web crippling is shown in Figs. 5 and 6.

The boundary conditions and loading were carefully simulated in the finite element models. In the tests the Z-specimens setup was hinged roller simple beams. In the finite element models, the same boundary conditions were simulated by restraining the vertical, lateral and longitudinal movements of flange nodes at hinge support while at roller support the longitudinal movement of flange nodes was released and vertical and lateral movements were restrained as shown in Fig. 5.

Furthermore, in the tests the movement of the loading jack was only allowed vertically up and downward with no rotation or lateral movement allowed. The same conditions were simulated in the finite element models by restraining the lateral movement of the top flange nodes at the intersection line between the top flange and the rounded corner of the web along the loading plate length as shown in Fig. 6.

The loading simulation in the finite element models was carefully selected. It was observed in tests that, after placing the loading plate on the top flange and once the test loading process start, the top flange rotates, the contact between the loading plate and top

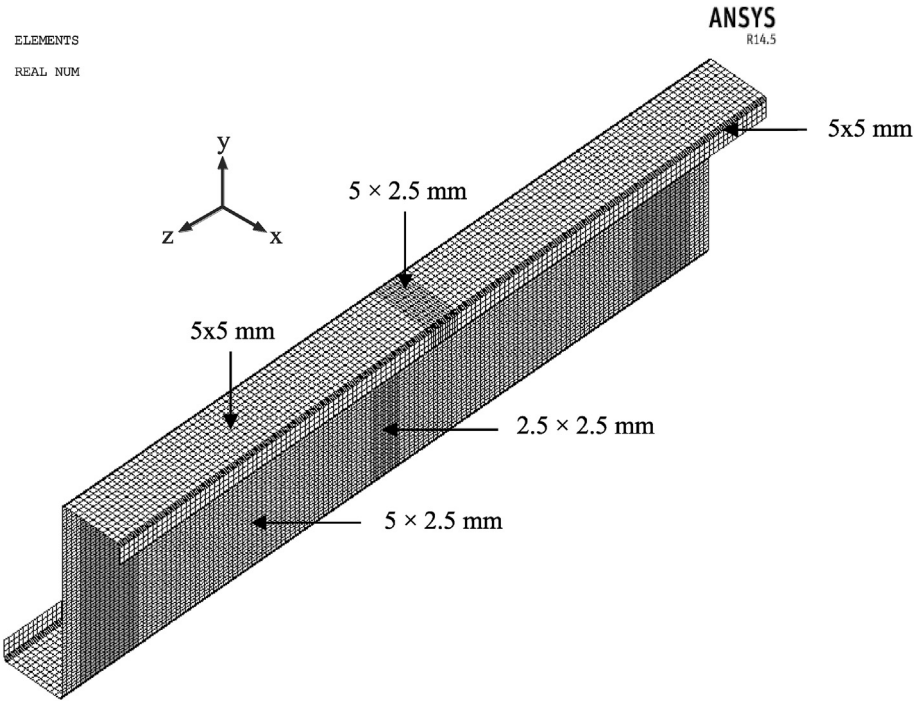

Fig. 5. Typical meshing arrangement in finite element models.

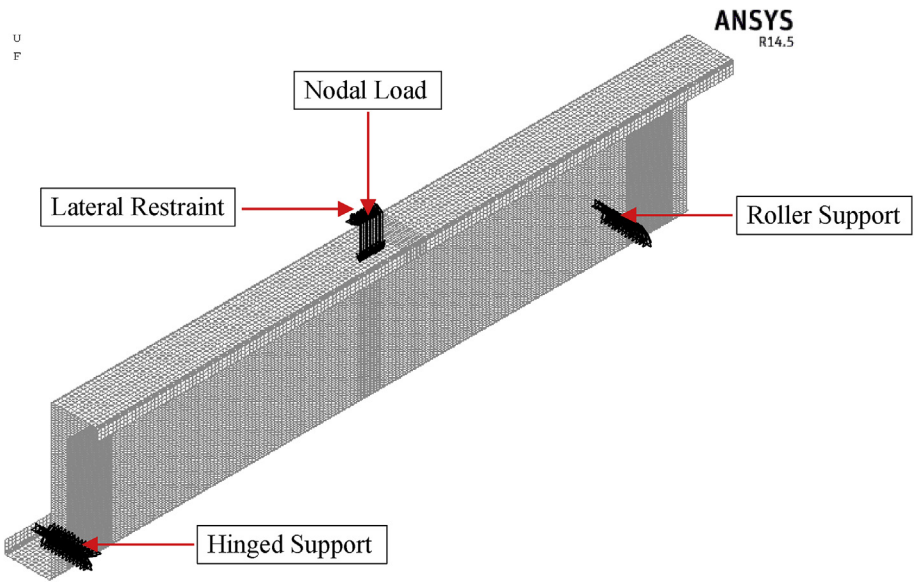

Fig. 6. Finite element models, loading pattern and boundary conditions.

flange surface is lost and the loading plate is supported on the line of intersection between the top flange and rounded corner of the web. Accordingly, in finite element modeling the test load was simulated as a nodal load applied on the nodes at the intersecting line between the top flange and rounded web corner. This type of loading simulation was adopted in Ref. [19].

In the current finite element analysis, the material properties and nonlinearity has been simulated on bases of the measured coupon test results presented in Table 2 by applying the idealized model proposed by **Abdel-Rahman and Sivakumaran** [17] for stress strain relationship considering that, young's modulus $E = 210000\ N/mm^2$ and passion ratio $\upsilon = 0.3$. The large strain behavior of the material was implemented using the multilinear isotopic hardening material model. Fig. 7 shows the idealized stress strain curves adopted in the finite element models analysis for the conducted three coupon tests.

The idealized stress strain curves are defined through five segment lines as following; the first line segment extends from zero to ($0.75F_y$) on stress axis with slop equals to young's modulus (E). The second line segment extends to stress ($0.875F_y$) with slop equals to (E/2). The third line segment extends to stress value equals (F_y) and has a slop equals to (E/10). The fourth line segment has slop equals to (E/200) up to the ultimate stress (F_u). The last segment has zero slop and extend to the ultimate strain (ε_u).

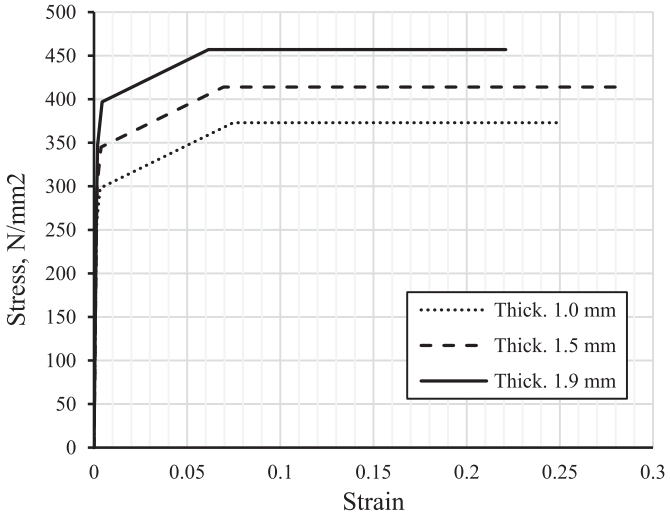

Fig. 7. Idealized stress strain curves for the three coupon tests.

Figs. 8 and 9 show sample of the finite element analysis results for stiffened and un-stiffened specimens respectively. The shown stresses distribution are plotted at the ultimate loads and failure loads. The finite element models have been validated against the experimental work by means deformed shapes, ultimate loads and load displacement curves. Fig. 10 shows the agreement between the deformed shape from test and finite element analysis.

Table 3, shows that the predicted ultimate loads from finite element analysis are in a good agreement with the measured tests ultimate loads. The statistics shows that the mean value of the predicted finite element ultimate loads to the test ultimate loads equals to 1.03 and the coefficient of variation COV = 0.02. Fig. 11, shows the load displacement curves from both finite element analysis and the test results. The figure shows how results are matching well.

5. Analytical model

This analytical model has been developed based on the good agreement noticed between the deformed shapes from experiments as well as from the finite element models as shown in Fig. 10. Fig. 12 shows the deformed shape through the flat web height at mid span of finite element models. The deformed shape has been plotted at three different loading increments. It is observed that, the maximum deformation occurs at about one third the flat web height which is similar to the deformed shape of a simply supported plate with elastic rotational restraint at its lower edge, as shown in Fig. 12.

Based on this similarity, the flat web of cold formed steel Z-section can be idealized as, a rectangular thin plat simply supported on its vertical sides and top edge and elastically restrained against rotation at the bottom edge, as shown in Fig. 13. The elastic rotational restrain at the bottom edge of the idealized plate is provided by the rotational stiffness of the bottom flange and the adjacent parts beyond the flat web height. The idealized thin plate is subjected to locally distributed in-plan edge compressive force **P** and bending moment $\mathbf{M_o}$. The applied stresses are assumed to spread

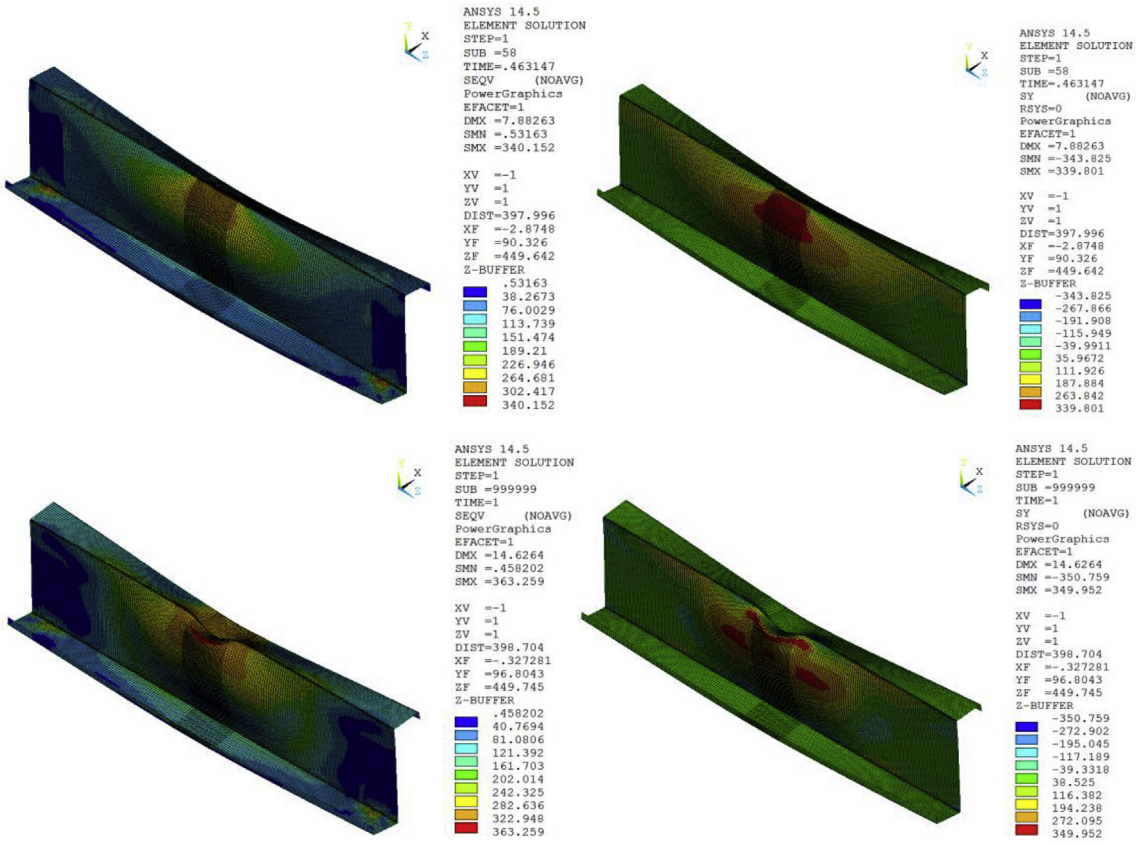

Fig. 8. Sample of finite element analysis results for stiffened specimen Z204 × 62 × 16 × 1.5-R2.0-N100.

downward through the web height at an angle 45° beyond the loading plate width till the location of the maximum out of plan displacement as shown in Fig. 13.

The deformed shape along the plate width is assumed to follow a sin curve with maximum displacement amplitude (***a***) at the mid width as shown in Fig. 13. The rotational stiffness $\boldsymbol{K_t}$ at the bottom edge of the idealized thin plate is equivalent to the torsional stiffness of a fixed-fixed beam of span (L), with a concentrated twisting moment at mid span; accordingly, it can be calculated according to the following expression.

$$K_t = \frac{4\,G\,J}{L} \tag{7}$$

where:

a Maximum out of plan displacement, mm
B Plate width at the location of maximum out of plane displacement, Fig. 13
e The eccentricity of the applied load = (R + t/2) mm
E Young's modulus of steel, = 210 kN/mm2
Fy Steel yield stress, kN/mm2
G Shear modulus of steel = 81 kN/mm2
h Flat web height, mm
I Second moment of area of the effective web section = B t3/12, mm4
J Torsion constant for lipped flange = (ds + b −4 (R + t) + π (R + t/2)) t3/3 mm4
L Equivalent Beam span for torsional rigidity = N+2 h
Mo Moment due to eccentric applied load = (P e) kN.mm
N Bearing plate width, mm
P The applied load, kN
t Web thickness, mm

For the previously described boundary conditions and loading pattern, the idealized web plate has the following deformed shape and bending moment equations:

$$\theta(y) = \frac{M_o h}{EI}\left(\frac{1}{2}(1+C)\left(\frac{y}{h}\right)^2 - C\left(\frac{y}{h}\right) - (1-2C)\right) \tag{8.a}$$

$$w(y) = \frac{M_o h^2}{6EI}\left((1+C)\left(\frac{y}{h}\right)^3 - 3C\left(\frac{y}{h}\right)^2 - (1-2C)\left(\frac{y}{h}\right)\right) \tag{8.b}$$

$$M(y) = M_o\left((1+C)\frac{y}{h} - C\right) \tag{8.c}$$

where; θ(y), w(y), and M(y) are the slopes, deflection and bending moment along the web height. The factor C represents the relative stiffness of the web plate to the torsional stiffness of the flange, where its value is given by the following expression:

$$C = \frac{0.5}{1 + \frac{3EI}{K_t.h}} \tag{9.a}$$

The value of (C) ranges from 0 to 0.5, where the two extreme cases represent hinge-hinged condition (C = 0), and Fixed-hinged condition (C = 0.5). the deformed shape and bending moment distribution over the plate height are shown in Fig. 13.

The maximum out of plan displacement (***a***) corresponds to a slope of zero value, which takes place at a height between $h/\sqrt{3}$ and ***2 h/3*** which are the extreme values for the elastically restrained edge in case of hinged and fixed edges respectively. Accordingly, the most stressed section is considered to be at the maximum

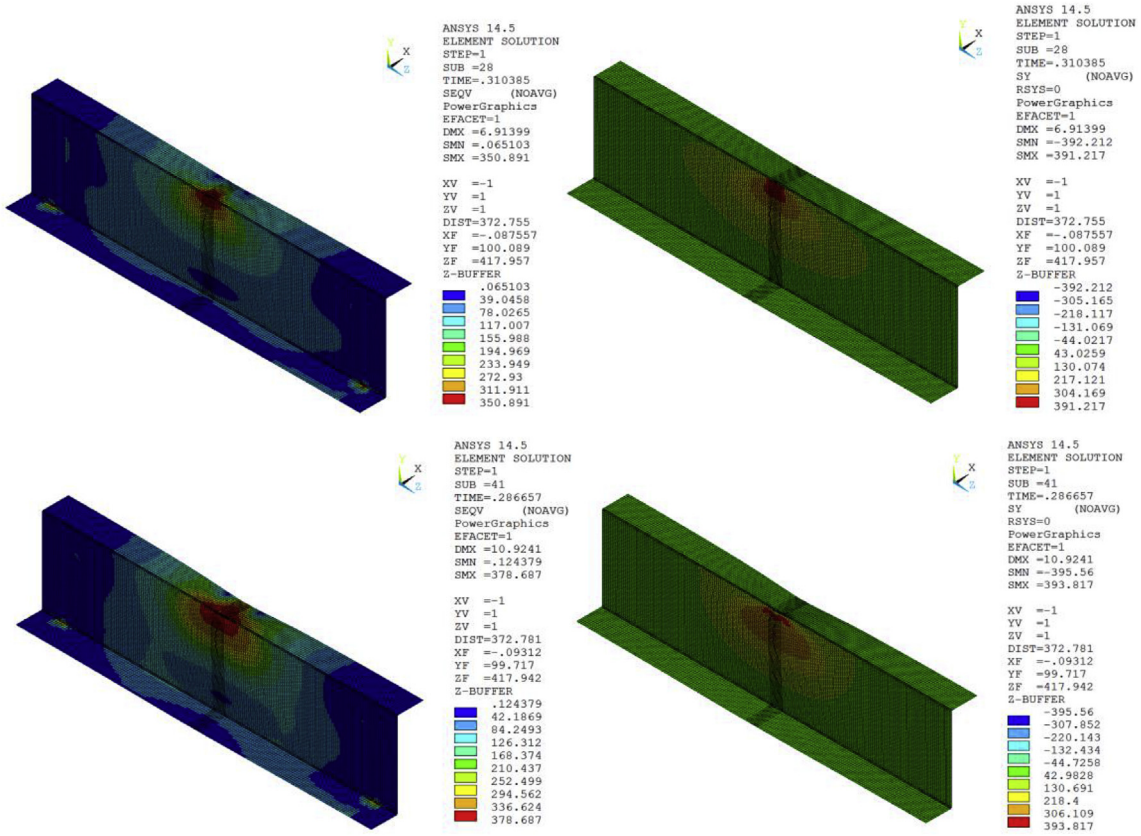

Fig. 9. Sample of finite element analysis results for un-stiffened specimen Z204 × 62 × 16 × 1.5-R2.0-N100.

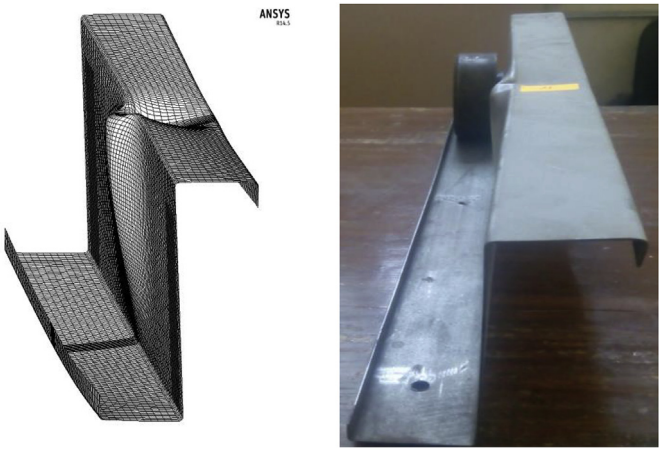

(a) (b)

Fig. 10. Deformed shape of test specimen Z150 × 62 × 16 × 1.5-R2.0-N30 according to: (a) Finite Element Analysis & (b) Experimental Work.

deformed shape location. The applied loads is assumed to spread through the web height at 45° angle on both sides of the loading plate. According to this assumption, the effective web width ***B*** at the critical section is given by the following expression:

$$B = N + 2(h - y) \cong N + 0.8\,h \tag{9.b}$$

As can be noticed from Fig. 8, the straining actions affecting the most critical section are;

Table 3
Web crippling ultimate loads from tests and finite element analysis.

Test Specimen	P_t, kN	P_{FE}, kN	P_{FE}/P_t
Z150 × 62 × 16 × 1.5-R2.0-N30	6.92	6.96	1.01
Z202 × 60 × 00 × 0.9-R2.0-N30	1.91	2.39	1.25
Z204 × 62 × 16 × 1.4-R2.0-N30	6.65	5.98	0.90
Z204 × 64 × 16 × 1.9-R2.0-N30	12.51	13.71	1.10
Z204 × 62 × 00 × 1.5-R2.0-N30	6.84	6.73	0.98
Z204 × 62 × 16 × 1.4-R2.0-N50	7.78	6.75	0.87
Z204 × 60 × 00 × 1.5-R2.0-N50	7.98	7.93	0.99
Z204 × 62 × 16 × 1.5-R2.0-N100	9.60	9.50	0.99
Z202 × 62 × 00 × 1.4-R2.0-N100	8.37	8.29	0.99
Z254 × 62 × 16 × 1.5-R2.0-N30	7.85	6.84	0.87
Z202 × 62 × 16 × 1.1-R2.0-N30	3.08	3.62	1.18
Z203 × 62 × 16 × 1.0-R2.0-N100	4.35	5.27	1.21
Mean			1.03
COV			0.02

a) The applied load ***P***, which produce uniform axial compression of the web plate thickness.
b) The moment resulting from its eccentricity ***M(y)***, which produces compressive stress on one face and tensile stress on the other face.
c) An additional moment due to the second order effect $\mathbf{M_{add}}$, that can be calculated by integrating the applied line load at the critical section (P/B) multiplied by the corresponding out of plan displacement $\left(\boldsymbol{a}\,\mathbf{sin}\,\frac{\pi x}{B}\right)$ as follows:

$$M_{add} = \frac{P}{B}\int_{x=0}^{B} a \sin\frac{\pi x}{B}\,dx = \frac{2P\,a}{\pi} \tag{10.a}$$

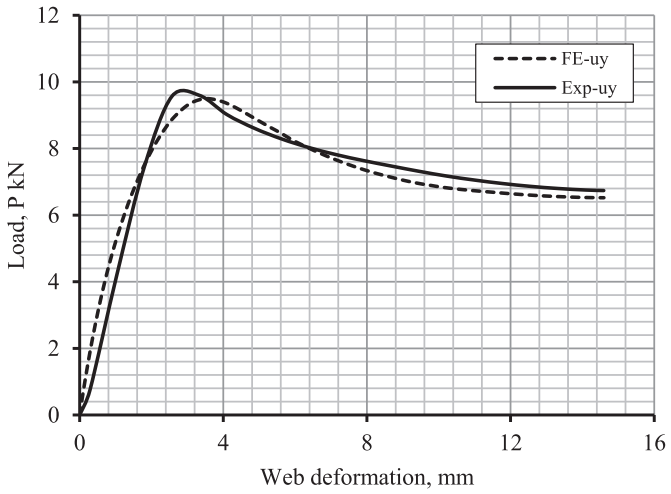

Fig. 11. Load displacement curves for Z04 × 62 × 16 × 1.4-R2.0-N100 according to: Finite Element Analysis & Experimental Work.

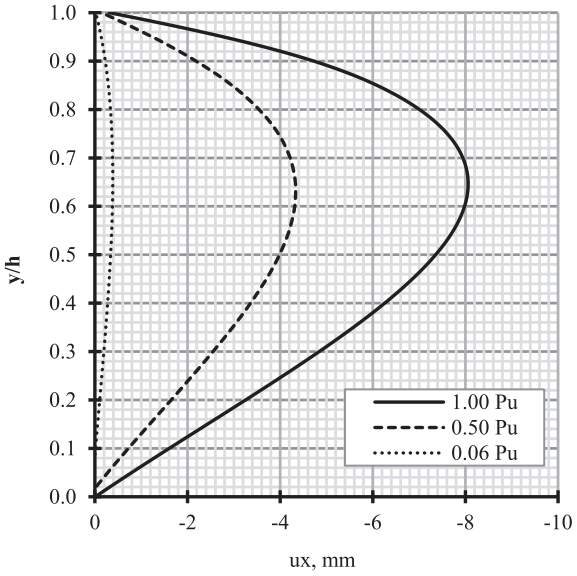

Fig. 12. Flat web deformed shape at mid span of finite element models at three stages; 0.06, 0.5 and 1.00 of the ultimate FE load.

d) An additional moment due to web initial imperfection, which is given by:

$$M_i = P\,\delta_i \tag{10.b}$$

At the critical section, the total normal stress is resulting from the axial load ***P***, and the total bending moment ***M***. The two stress components are given by the following expressions:

$$F_a = \frac{P}{B\,t} \tag{11.a}$$

$$F_b = \frac{4M}{B\,t^2} \tag{11.b}$$

where, $\boldsymbol{F_a}$ and $\boldsymbol{F_b}$ are the two stress components resulting from axial load and bending moment respectively. According to the first yield failure criteria, the failure occurs when the total stresses reach the yield stress of material, then; the following expressions can be formed:

$$\frac{P}{B\,t} + \frac{4M}{B\,t^2} = F_y \tag{12}$$

In equation (12), the total bending moment ***M*** represents the contribution of; the applied bending moment (M(y), equation (8.c)), the second order moment (M_{add}, equation (10.a)), and the bending moment resulting from initial imperfection (M_i, equation (10.b)). The initial imperfection (δ_i) is usually considered as a percentage of the web depth, a practical range of h/250 to h/1000 can be reasonably assumed. Effect of initial imperfection on web crippling strength will be studied later on, however, a value of h/500 can be considered in the model derivation. Therefore the total bending moment on the most critical section is given by the following expression:

$$M = M_o\left((1+C)\frac{y}{h} - C\right) + \frac{2P\,a}{\pi} + P\frac{h}{500} \tag{13}$$

The value of (***a***), represents the maximum displacement amplitude resulting from the bending moment diagram shown in Fig. 8. This value can be obtained by equating the slope (θ(y)) of equation (8.a) to zero, to obtain the value of y corresponding to the maximum value of (w(y)), then the value of (***a***) can be obtained from equation (8.b).

The plate maximum lateral deflection occurs at a height of $\boldsymbol{y = h/\sqrt{3}}$ (0.58 h) for the simply supported boundary conditions, and $\boldsymbol{y = 2h/3}$ for the fixed hinged boundary condition. For the general case of elastically restrained boundary condition, the maximum

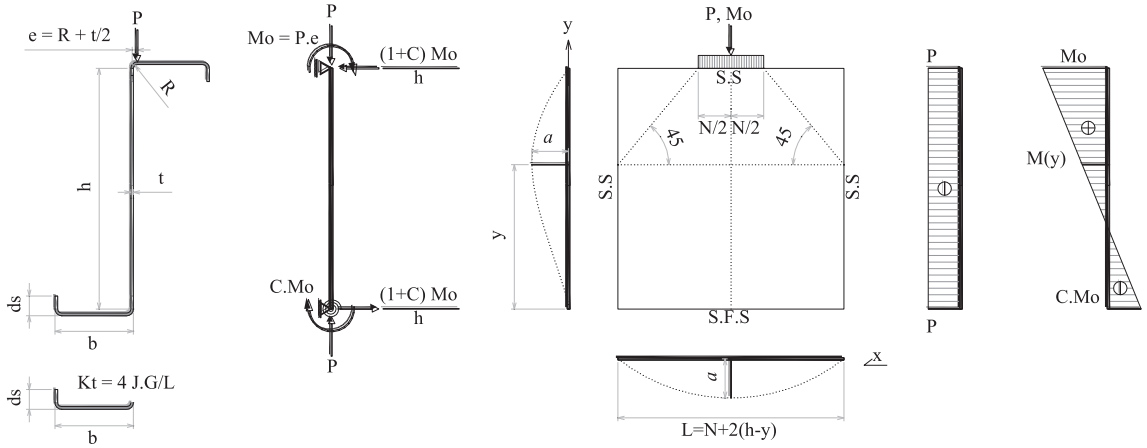

Fig. 13. Proposed plate model for web crippling of Z-section under IOF loading conditions.

Table 4
Test specimens' parameters and web crippling ultimate loads.

Test Specimen	t, mm	F_y, N/mm^2	h/t	N/t	R/t	P_t, kN	P_{FE}, kN	$P_{Eq\ (18)}$, kN	P_{EN}, kN	P_{AISI}, kN	P_{FE}/P_t	$P_{Eq\ (18)}/P_t$	P_{EN}/P_t	P_{AISI}/P_t
Z150 × 62 × 16 × 1.5-R2.0-N30	1.5	345	95.3	20.0	1.33	6.92	6.96	7.32	9.78	10.87	1.01	1.06	1.41	1.57
Z202 × 60 × 00 × 0.9-R2.0-N30	0.9	298	218.0	33.3	2.22	1.91	2.39	2.19	2.62	2.21	1.25	1.15	1.37	1.48
Z204 × 62 × 16 × 1.4-R2.0-N30	1.4	345	140.9	21.4	1.43	6.65	5.98	7.49	7.92	9.25	0.90	1.13	1.19	1.39
Z204 × 64 × 16 × 1.9-R2.0-N30	1.9	398	103.3	15.8	1.05	12.51	13.71	13.59	16.70	19.94	1.10	1.09	1.33	1.59
Z204 × 62 × 00 × 1.5-R2.0-N30	1.5	345	131.3	20.0	1.33	6.84	6.73	7.42	9.22	8.15	0.98	1.08	1.35	1.19
Z204 × 62 × 16 × 1.4-R2.0-N50	1.4	345	140.9	35.7	1.43	7.78	6.75	7.09	8.61	10.31	0.87	0.91	1.11	1.33
Z204 × 60 × 00 × 1.5-R2.0-N50	1.5	345	131.3	33.3	1.33	7.98	7.92	8.15	9.97	8.88	0.99	1.02	1.25	1.11
Z204 × 62 × 16 × 1.5-R2.0-N100	1.5	345	131.3	66.7	1.33	9.60	9.50	10.08	10.58	12.26	0.99	1.05	1.10	1.28
Z202 × 62 × 00 × 1.4-R2.0-N100	1.4	345	139.4	71.4	1.43	8.37	8.29	8.64	10.61	8.83	0.99	1.03	1.27	1.05
Z254 × 62 × 16 × 1.5-R2.0-N30	1.5	345	164.7	20.0	1.33	7.85	6.84	7.56	8.70	10.50	0.87	0.96	1.11	1.34
Z202 × 62 × 16 × 1.1-R2.0-N30	1.1	298	178.0	27.3	1.82	3.08	3.62	3.47	4.20	4.85	1.18	1.13	1.36	1.57
Z203 × 62 × 16 × 1.0-R2.0-N100	1.0	298	197.0	100.0	2.00	4.35	5.27	3.77	5.14	5.39	1.21	0.87	1.18	1.24
Mean											1.03	1.04	1.25	1.35
COV											0.02	0.008	0.01	0.03

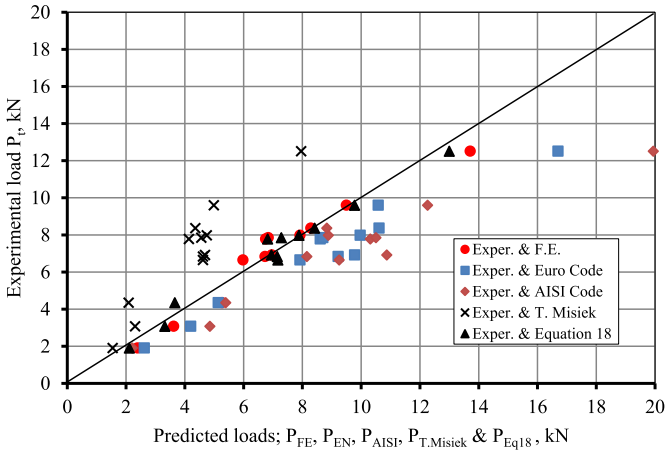

Fig. 14. Comparisons of experimental ultimate loads and predicted loads from finite element models, proposed analytical equation and Codes design approach.

displacement can be assumed to take place at $\boldsymbol{y = 0.6\,h}$ for simplicity. Then, the total maximum moment given by equation (13) can be re-expressed as follows:

$$M = P\,h \Big/ 500 + (0.6 - 0.4\,C)(R + t/2)P + \frac{(R + t/2)\,(0.128 - 0.112\,C)(h)^2}{\pi\,EI}P^2 \tag{14}$$

Substituting $\boldsymbol{M}$ from equation (14) into equation (12) and rearranging the different terms, results in the following expression:

$$\left[(0.512 - 0.448C)\left(\frac{R}{t} + 0.5\right)\frac{(h)^2}{\pi\,EI}\right]P_n^2 + \left[1 + \frac{4h/t}{500} + (2.4 - 1.6C)\left(\frac{R}{t} + 0.5\right)\right]P_n - P_y = 0 \tag{15}$$

where, $\boldsymbol{P_n}$ is the value of applied load that causes failure due to local web yielding (web crippling), which represents the nominal capacity of a section undergoing web crippling. $\boldsymbol{P_y}$, is the squash load of the effective portion of the web that is given by the following expression:

$$P_y = B\,t\,F_y \tag{16}$$

Equation (15), can be simplified to the following form:

$$\alpha\,P_n^2 + \beta\,P_n - P_y = 0 \tag{17}$$

Equation (17) can be solved to obtain the web crippling nominal failure load P_n. P_n can be given by the following expression:

$$P_n = \frac{1}{2\alpha}\left[\sqrt{\beta^2 + 4\alpha\,P_y} - \beta\right] \tag{18}$$

where, P_y is given by equation (16), and α and β are given by the following expressions:

$$\alpha = (0.512 - 0.448C)\left(\frac{R}{t} + 0.5\right)\frac{(h)^2}{\pi\,EI} \tag{19.a}$$

$$\beta = 1 + \frac{4h/t}{500} + (2.4 - 1.6C)\left(\frac{R}{t} + 0.5\right) \tag{19.b}$$

Equation (18) gives the nominal web crippling load in terms of the material properties E and F_y, bearing length N, geometrical properties of the cross section h, R and t. A value of h/500 is considered as a web initial imperfection in equations (18) and (19).

6. Results

In this section, the nominal web crippling capacities predicted by equation (18) (P_n) have been compared to the experimental ultimate loads (P_t), the finite element ultimate loads (P_{FE}), the Eurocode web crippling resistances (P_{EN}) and the nominal strengths estimated by the North American specification (P_{AISI}). Table 4 presents the web crippling parameters for each test specimen in addition to the ultimate loads according to tests, finite element analysis, analytical model (for initial imperfection of h/500), and the ultimate resistance or nominal

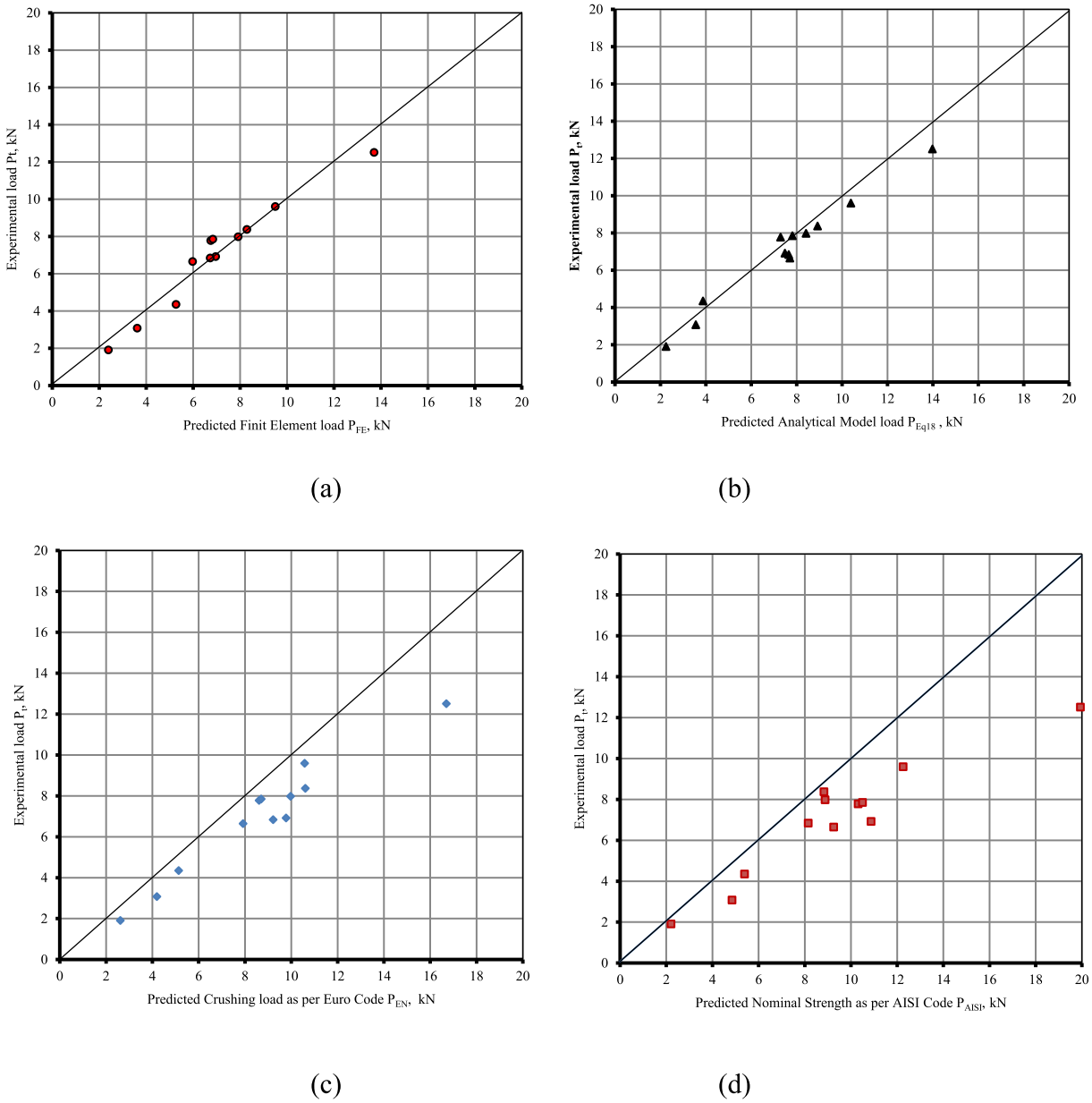

Fig. 15. Comparison between; (a) Finite element ultimate load and experimental ultimate load, (b) Analytical model predicted load and experimental ultimate load, (c) Eurocode resistance load and experimental ultimate load and (d) North American Code nominal strength and experimental ultimate load.

Table 5
Initial imperfection effect on the predicted web crippling ultimate loads.

Test Specimen	t (mm)	Fy (N/mm^2)	Test Result Pt (kN)	Analytical Model Result for different values of Si					
				0	h/1000	h/500	h/250	h/150	h/100
Z150x62xl6xl.5-R2.0-N30	1.50	345.00	6.92	7.71	7.51	7.32	6.95	6.51	6.00
Z202x60x00x0.9- R2.0- N 30	0.90	298.00	1.91	2.30	2.24	2.19	2.09	1.97	1.82
Z204x62xl6xl.4-R2.0-N30	1.40	345.00	6.65	7.91	7.69	7.49	7.10	6.64	6.11
Z204x64xl6xl.9-R2.0-N30	1.90	398.00	12.51	14.35	13.95	13.59	12.89	12.04	11.08
Z204x62x00xl.5-R2.0-N30	1.50	345.00	6.84	7.84	7.62	7.42	7.04	6.58	6.06
Z204x62xl6xl.4-R2.0-N50	1.40	345.00	7.78	7.48	7.28	7.09	6.74	6.30	5.81
Z204x60x00xl.5-R2.0-N50	1.50	345.00	7.98	8.61	8.36	8.15	7.74	7.24	6.67
Z204x62xl6xl.5-R2.0-N 100	1.50	345.00	9.60	10.66	10.34	10.08	9.57	8.95	8.25
Z202x62x00xl.4-R2.0-N 100	1.40	345.00	8.37	9.13	8.86	8.64	8.22	7.70	7.11
Z254x62xl6xl.5-R2.0-N30	1.50	345.00	7.85	7.99	7.77	7.56	7.18	6.70	6.16
Z202x62xl6xl.l-R2-N30	1.10	298.00	3.08	3.65	3.56	3.47	3.29	3.08	2.84
Z203x61x16x1.0-R2-N100	1.00	298.00	4.35	3.97	3.87	3.77	3.60	3.38	3.13

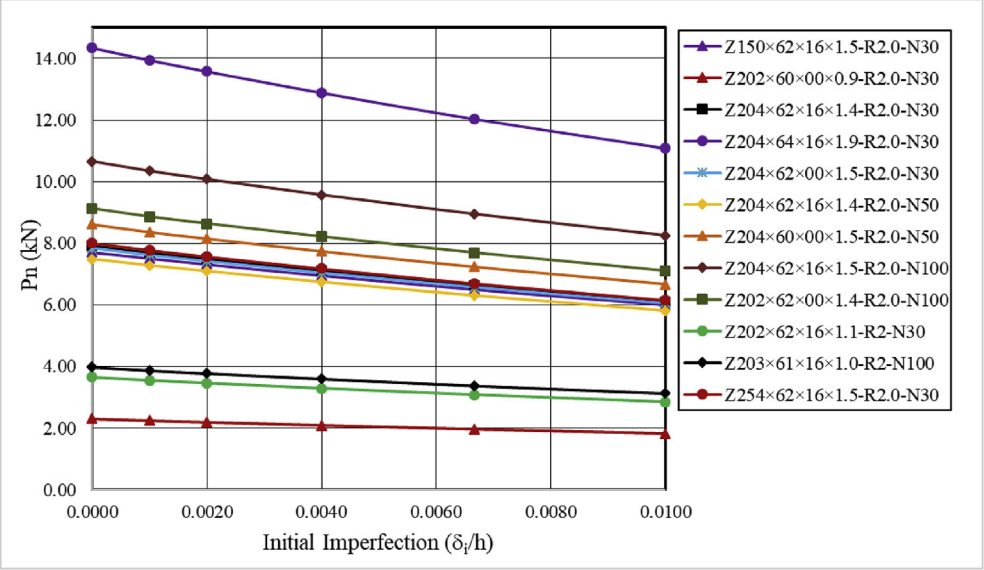

Fig. 16. Variation of ultimate web crippling resistance with initial web imperfection for all studied sections.

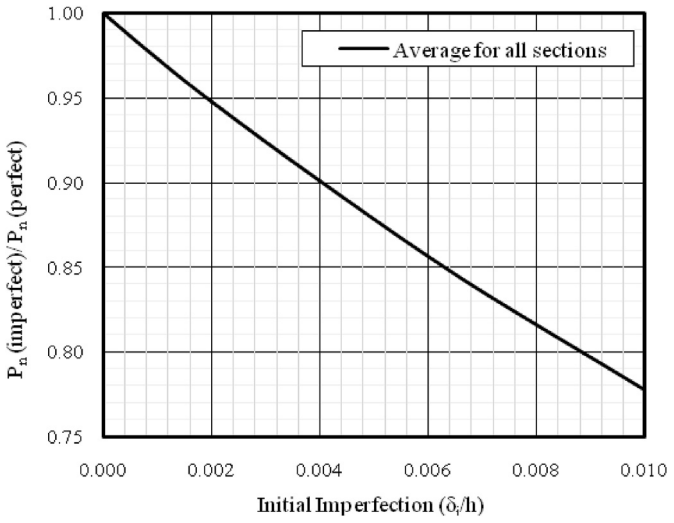

Fig. 17. Variation of average web crippling strength reduction with initial web imperfection for all studied sections.

strength according to the design codes.

Fig. 14 shows a comparison between the experimental web crippling ultimate loads on the vertical axis (P_t) and the strengths predicted by the other different methods on the horizontal axis. The comparison shows the values obtained from; the finite element analyses (P_{FE}), the analytical model ($P_{Eq\ (18)}$) utilizing equation (18), the nominal strengths as per AISI (P_{AISI}), and the resistances calculated as per the Eurocode (P_{EN}) versus the experimental ultimate resistance (P_t).

For more convenience, comparison between each individual approaches and the experimental results are shown in Fig. 15. From the comparisons shown in Table 4, Figs. 14 and 15 it can be concluded that, the ultimate load predicted by the finite element is slightly higher than the load obtained from the tests (higher by 3%). The proposed analytical model (equation (18)) compares well with both experimental and finite element results. The average strength of the developed model is 4% higher than the average test strength, with a variance of 0.008. The average strength obtained by the analytical model is 2% higher than the average resistance obtained by the finite element method with a variance of 0.016.

On the other hand, the comparisons between test loads and designs codes showed that, the North American specification and the Eurocode overestimate the web crippling capacity by 35%, and 25% respectively.

Accordingly, the developed analytical model can be used as a simple, but rational, design approach. The model predicts the ultimate web crippling accurately using a simple equation (equation (18)). On the other hand, the expressions used by the design codes of practice overestimate the web crippling resistance for the Z-section, and further adjustments need to be introduced to these expressions. However, this issue will be studied in another research.

The developed analytical model equation (18) is also applied to investigate the effect of initial web imperfection on the ultimate resistance of web crippling. Web crippling resistance has been calculated for all studied sections under different values of initial imperfection, $\delta_i = 0$, h/1000, h/500, h/250, h/150 and h/100.

Table 5 shows the effect of the initial web imperfection on the predicted web crippling strength as per the proposed analytical model for each test specimen in addition to the ultimate loads according to tests.

Fig. 16 shows the variation of ultimate web resistance with initial imperfection (δ_i/h) for all sections. Fig.17 shows the variation of average strength reduction of all sections with the values of initial web imperfection.

From Table 5 and Figs. 16 and 17, it can be concluded that; the presence of a practical level of initial imperfection (h/500), reduces the web crippling resistance by about 6%. Increasing initial imperfection value to (h/100) results in a strength reduction of about 22.5%

7. Conclusions

In this research, a simple but rational analytical model has been developed to predict the nominal web crippling strength of cold formed Z-sections. Results of the proposed model were validated by comparison with experimental results, finite element analysis and codes design approach. Based on the results of these comparisons, the following remarks can be concluded:

The developed analytical model (equation (18)), can be considered as simple and accurate tool for estimating the web crippling nominal strength for cold formed steel Z-sections. The developed

model is capable to account for the effect of initial web imperfection. The developed analytical model results agree well with the experimental result, with an average difference of 4% and with a variance of 0.008.

Results of the model also are in a very good agreement with the finite element results obtained using ANSYS software. The average difference between the developed model results and finite element analysis is 3%, with a variance of 0.016. This means that, the developed model is a reliable tool to predict web crippling resistance of Z-sections.

The design codes included in this study are not conservative for estimating the web crippling nominal strengths compared to both finite element and experimental results. Further adjustments are recommended to be applied for the studied codes design approach, however, this will be thoroughly investigated in another research.

Declaration of interest

None.

Appendix ASupplementary data

Supplementary data to this article can be found online at https://doi.org/10.1016/j.jcsr.2019.105813.

References

[1] W.W. Yu, R.A. LaBoube, Cold-Formed Steel Design, fourth ed., John Willey & Sons. INC., U.S.A., 2010.

[2] B. Young, G.J. Hancock, Cold-formed steel channels subjected to concentrated bearing load, J. Struct. Eng. 129 (8) (August, 2003).

[3] B. Young, G.J. Hancock, Design of cold-formed channels subjected to web crippling, J. Struct. Eng. 127 (10) (October, 2001).

[4] W.X. Ren, S.E. Fang, B. Young, Analysis and design of cold-formed steel channels subjected to combined bending and web crippling, J. Thin-Walled Struct. 44 (2006) 314–320.

[5] M. Bakker, J. Stark, Theoretical and experimental research on web crippling of cold-formed flexural steel members, J. Thin-Walled Struct. 18 (1994) 261–290.

[6] Y. Chen, X. Chen, C. Wang, Experimental and finite element analysis research on cold-formed steel lipped channel beams under web crippling, J. Thin-Walled Struct. 87 (2015) 41–52.

[7] M. Dara, C. Yu, Direct strength method for web crippling of cold- formed steel C- and Z- sections subjected to one-flange loading, J. Steel Struct. Constr. 1 (2015) 105.

[8] B. Beshara, R. Schuster, Web Crippling Data and Calibrations of Cold Formed Steel Members, Research Report RP00-2, Canadian Cold Formed Steel Research Group, University of Waterloo, Canada, 2000 (AISI Report, Revised 2006).

[9] R.R. Gerges, R.M. Schuster, Web crippling of single web cold formed steel members subjected to end one-flange loading, in: Fourteenth International Specialty Conference on Cold-Formed Steel Structures, Missouri U.S.A., St. Louis, October 15-16, 1998.

[10] M. Macdonald, M.A. Heiyantuduwa, A design rule for web crippling of cold-formed steel lipped channel beams based on nonlinear FEA, J. Thin-Walled Struct. 53 (2012) 123–130.

[11] P. Natário, N. Silvestre, D. Camotim, Computational modeling of flange crushing in cold-formed steel sections, J. Thin-Walled Struct. 84 (2014) 393–405.

[12] J. Rhodes, D. Nash, An investigation of web crushing behavior in thin-walled beams, J. Thin-Walled Struct. 32 (1998) 207–230.

[13] American Iron and Steel Institute (AISI), "North American Specification for the Design of Cold-Formed Steel Structural Members", AISI S100-16, Washington, DC, U.S.A.

[14] CEN European Committee for Standardization, EN 1993-1-3:2006, Euro Code 3: Design of Steel Structures Part 1-3: General Rules - Supplementary Rules for Cold Formed Members and Sheeting, CEN, Brussels, Belgium, 2006.

[15] ANSYS 14.5, User's Manual. Swanson Analysis System, U.S.A., 2012.

[16] M.S. Soliman, A.B. Badawy Abu-Sena, E.E. Darwish, M.S. Saleh, Resistance of cold-formed steel sections to combined bending and web crippling, Ain Shams Eng. J. 4 (2013) 435–453.

[17] N. Abdel-Rahman, K.S. Sivakumaran, Evaluation and Modeling of the Material Properties for Analysis of Cold-Formed Steel Sections, in: International Specialty Conference on Cold-Formed Steel Structures. Paper 3, October 17, 1996.

[18] W.X. Ren, S.E. Fang, B. Young, Finite-element simulation and design of cold-formed steel channels subjected to web crippling, J. Struct. Eng. 132 (12) (December 1, 2006).

[19] A.P.C. Duarte, N. Silvestre, A new slenderness-based approach for the web crippling design of plain channel steel beams, Int. J. Steel Struct. 13 (3) (September 2013) 421–434.

[20] T. Misiek, A. Belica, Calibration of European web-crippling equations for cold-formed C- and Z-sections, J. Steel Constr. (1) (December 2019).

[21] Lavan Sundararajah, Mahen Mahendran, Pologanathan Keerthan, New design rules for lipped channel beams subject to web crippling under two-flange load cases, Thin-Walled Struct. 119 (2017) 421–437.

[22] Lavan Sundararajah, Mahen Mahendran, Pologanathan Keerthan, Web crippling experiments of high strength lipped channel beams under one-flange loading, J. Constr. Steel Res. 138 (2017) 851–866.

[23] Y. Lian, A. Uzzaman, J.B.P. Lim, G. Abdelal, D. Nash, B. Young, Effect of web holes on web crippling strength of cold-formed steel channel sections under end-one-flange loading condition - Part I: tests and finite element analysis, Thin-Walled Struct. 107 (2016) 443–452.

[24] Y. Lian, A. Uzzaman, J.B.P. Lim, G. Abdelal, D. Nash, B. Young, Web crippling behaviour of cold-formed steel channel sections with web holes subjected to interior-one-flange loading condition-Part I: experimental and numerical investigation, Thin-Walled Struct. 111 (2017) 103–112.

[25] L. Sundararajah, M. Mahendran, P. Keerthan, Design of SupaCee sections subject to web crippling under one-flange load cases, J. Struct. Eng. 144 (2018), 04018222.